Robotica: (2019) volume 37, pp. 1804–1822. © Cambridge University Press 2019
doi:10.1017/S0263574719000274

A Multibody Dynamics Approach to Limit Cycle Walking

Jiawei He† and Gexue Ren‡*

†*Research Office, China Astronaut Research and Training Center, Beijing 100094, China.*
E-mail: hejw06@gmail.com
‡*School of Aerospace Engineering, Tsinghua University, Beijing 100084, China*

(Accepted February 27, 2019. First published online: April 10, 2019)

SUMMARY
Though significant efforts are made to develop mathematical models of the limit cycle walking (LCW), there is still a lack of a general and efficient framework to study the periodic solution and robustness of a complex model like human with knees, ankles and flat feet. In this study, a numerical framework of the LCW based on general multibody system dynamics is proposed, especially the impacts between the feet and the ground are modeled by Hunt–Crossley normal contact force and Coulomb friction force, and the modeling of the knee locking is presented as well. Moreover, event-based operating strategies are presented to deal with controls for the ground clearance and the knee locking. Importantly, a fast and efficient two-step algorithm is proposed to search for stable periodic gaits. Finally, maximum allowable disturbance is adopted as the index for stability analysis. All these features could be readily implemented in the framework. The presented solution is verified on a compass-like passive dynamic walking (PDW) walker with results in the literature. Based on this framework, a fairly complicated level-walking walkers with ankles and knees under control are analyzed and their periodic gaits are obtained, and surprisingly, double stable periodic gaits with, respectively, low speed and high speed are found.

KEYWORDS: Passive dynamic walking; Biped; Periodic gait; Stability.

1. Introduction

Passive dynamic walking (PDW) refers to the natural-looking walking that the passive mechanism demonstrates under only gravity.[1] Over the past several decades, PDW and extended limit cycle walking (LCW)[2] have been widely investigated. Such studies can gain better understanding of human walking, which can also help to develop efficient and robust walking mechanisms and exoskeletons.

Mathematical modeling is one of the effective ways to study LCW, whereas foot–ground impact is a major concerning. The majority of mathematical modeling is based on impact-based method,[3,4] whose dynamic models are discontinuous and rely on a number of assumptions. It assumes that walking is the process that one leg (the stance leg) attached to the ground at the contact point and another leg (the swing leg) swings in the air, and then the stance leg and the swing leg swap immediately when the swing leg impacts with the ground. It also assumes that the impact is finished instantaneous, inelastic and no slip. In other words, the walking consists of only single-foot-support phases which are divided by impacts. At the strike impact event, the governing equation and system states switch as the stance leg and the swing leg swap, resulting in discontinuity. The system state after an impact can be written as a function of system state before the impact by adopting the momentum theorem. Typical applications of this method include the simplest walking model,[5,6] compass-like PDW walker with flat foot,[7,8] four-link walker with ankles.[9] Though widely used, this method cannot study the impact process itself, the assumptions in this method may lead to artificial results and the modeling is difficult for sophisticated models[10,11] as the switch of system states is too complex. Moreover,

* Corresponding author. E-mail: rengx@mail.tsinghua.edu.cn

the impact-based method cannot model real human walking which includes both single-foot and double-feet-support phases.

Recently, a few studies[3,12] used force-based method for the impacts between the foot and the ground. The contact is dealt with norm contact force and friction force rather than a pivot joint in the impact-based method. In the force-based method, the system state is continuous and requires no special processing for impacts. Qi et al.[12] studied effects of elastic contact on the passive walking gait, whose results show that contact stiffness affects gait and walking stability significantly while contact damping and coefficient of friction have less influence. Koop and Wu[3] also used a similar contact model and LuGre friction model[13] to study a compass-like PDW walker. Correlation with the results of experiments shows that the force-based method can match the experimental results much better.[3] Compared to the impact-based method, the force-based method uses fewer assumptions and is capable of handling double-feet-support phase and providing details of impacts. However, the modeling of this method is more complex. It leads to more degree of freedoms (DOFs) of the system and thus more computation costs. And more importantly, the periodic gait is more difficult to find as the initial condition is always high dimensional, so available research based on this method is mainly for simple models. Therefore, there is still a lack of a general and efficient force-based method.

In the study of LCW, the stability is one of the most important feature and have been studied extensively. There are several stability indicators such as maximum Floquet multipliers, the basin of attraction (BoA),[6] Gait sensitivity norms,[14] maximum allowable disturbance.[1] An index of stability that has been most widely used is Floquet multipliers, which was eigenvalues of the Jacobian of application of Poincaré return map.[15] However, this index is based on infinitesimal deviations instead of finite disturbance, so it is called local stability. In contrast, global stability that includes the BoA and maximum allowable disturbance corresponds to finite disturbance, so it is more meaningful, but it costs much more computation, especially for a complex walker. Thus, an efficient framework is in need for the global stability analysis.

The purpose of this paper is to establish a systematic numerical framework of LCW based on the general multibody dynamics method. Within this framework, effective solution algorithms are proposed for finding the stable periodic gait and for robustness analysis. First, the impacts between the feet and the ground are modeled by Hunt–Crossley normal contact force and Coulomb friction force, which is adopted for modeling of knee locking as well. Second, event-based operating strategies are presented to deal with controls for the ground clearance, monitoring walking status, the knee locking and so on. Importantly, a fast and efficient two-step algorithm is proposed to search for initial conditions of the periodic gaits, which are highly dimensional. Finally, a maximum allowable disturbance indicator, which includes maximum allowable step-down height and step-up height, is adopted as the index for robustness analysis. All these features could be readily implemented in the multibody system, especially the control and the actuation can be easily incorporated. The presented solution framework is verified on a compass-like PDW walker by comparing results in the literature. Based on this framework, a fairly complicated level-walking walkers with ankles and knees are analyzed and their stable periodic gaits are obtained, and surprisingly, double stable periodic gaits with both low speed and high speed are found.

This paper is organized as follows. The modeling of LCW based on multibody dynamics is presented in Section 2. Section 3 presents the stable periodic gait searching algorithm and stability analysis solution. Section 4 gives details on the verification and application examples. Finally the summary is given in Section 5.

2. Multibody Dynamics Modeling of LCW

2.1. Governing equations

The general and efficient numerical framework presented here is based on multibody system dynamics. A multibody system[16,17] deals with the dynamics of a number of rigid bodies and flexible bodies which are connected by joints and/or force elements such as contacts, springs, controls and actuators and so on. Thus, multibody system dynamics is quite suitable for the study of LCW. Shown in Fig. 1(a–c) are three LCW walkers, respectively, the simple, intermediate and complex one. Though these models are quite different, the modeling procedures are the same under this framework. In the

https://doi.org/10.1017/S0263574719000274 Published online by Cambridge University Press

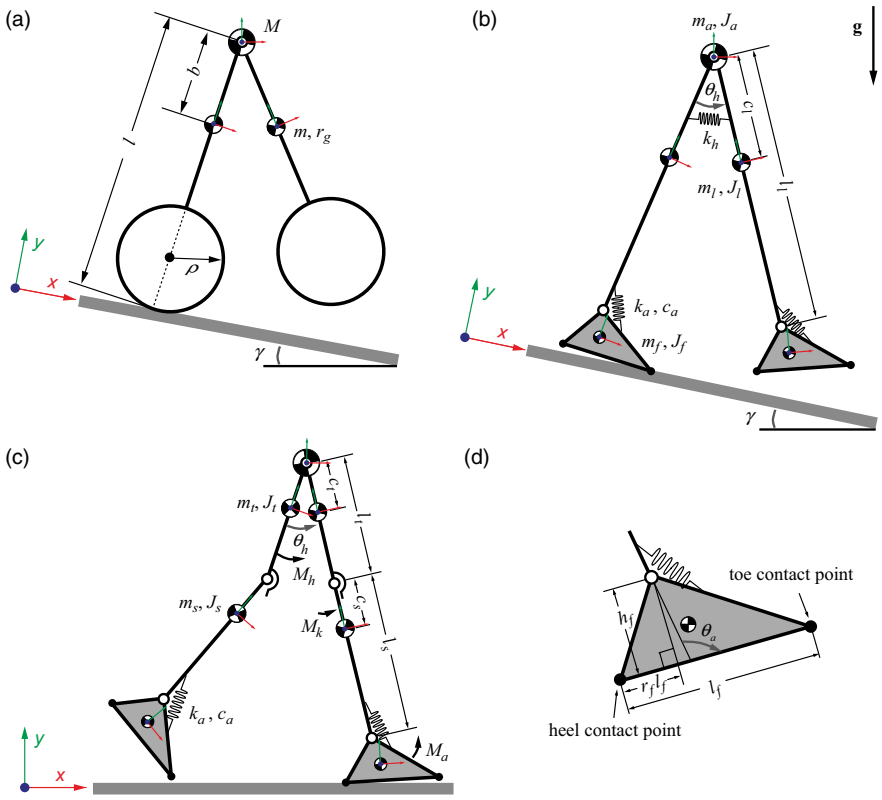

Fig. 1. (a) Schematic of a compass-like passive dynamic walker, (b) schematic of a PDW walker with flat feet and compliant ankles, (c) schematic of a level-walking model with ankles and knees and (d) schematic of a flat foot.

following, the second PDW walker with flat feet and compliant ankles is taken as an example to illustrate the modeling.

This model composes of five rigid bodies, that is, two legs, two feet and upper limb, whose center of mass is shown in Fig. 1(b). For simplicity, the torso is modeled as a lumped mass fixed to the hip. Both legs are hinged to the hip through revolute joints. A torsional spring is placed between two legs, which is introduced to adjust the walking frequency. Its torsional moment is $M_h = k_h\theta_h$, where θ_h is the angle between the two legs ($\theta_h > 0$ when left leg is ahead of right leg). Two feet are hinged to the two legs with revolute joints, respectively, and between each foot and its corresponding leg, there is a torsional spring with moment M_a. This model is placed on the slope with the angle γ and actuated by the gravity only. A two-dimensional model is considered here for simplicity, implemented by restricting the torso to the vertical plane (the xy plane) by a planar constraint. The x-axis is aligned with the slope.

For a multi-rigid body system consisting of N rigid bodies, the generalized coordinates of a rigid body[18] i ($i = 1, \ldots, N$, N is the number of rigid bodies) are expressed as $\mathbf{q}_i$. By employing the Lagrange equation of the first kind,[19] the general governing dynamic equations[18,20] of the general multibody system are established as

$$\begin{cases} \mathbf{M}\ddot{\mathbf{q}} + \dot{\mathbf{M}}\dot{\mathbf{q}} - \dfrac{\partial}{\partial \mathbf{q}}\left(\dfrac{1}{2}\dot{\mathbf{q}}^{\mathrm{T}}\mathbf{M}\dot{\mathbf{q}}\right) + \left(\dfrac{\partial \mathbf{C}}{\partial \mathbf{q}}\right)^{\mathrm{T}}\boldsymbol{\lambda} = \mathbf{Q} \\ \mathbf{C}(\mathbf{q}) = \mathbf{0} \end{cases} \tag{1}$$

where $\mathbf{Q} = \mathbf{Q}_g + \mathbf{Q}_c + \mathbf{Q}_e$ is the generalized forces that contain three parts, namely, $\mathbf{Q}_g$ is due to gravity, $\mathbf{Q}_c$ is due to the contact forces and $\mathbf{Q}_e$ is due to the external forces including torsional spring forces and active forces, $\mathbf{C}(\mathbf{q})$ is the general expression vector of constraint equations,[20] $(\partial \mathbf{C}/\partial \mathbf{q})^{\mathrm{T}}\boldsymbol{\lambda}$ represents the contribution of constraint forces and $\boldsymbol{\lambda}$ is the Lagrangian multiplier vector. The modeling of the contacts between the foot and the ground is very important and is presented in the following section.

https://doi.org/10.1017/S0263574719000274 Published online by Cambridge University Press

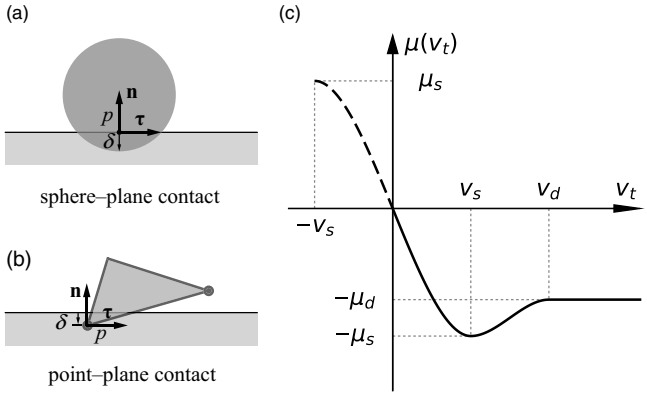

Fig. 2. Schematic of contact model: (a) sphere–plane contact, (b) point–plane contact, and (c) diagram of frictional coefficient.

2.2. Modeling of contact

In the force-based method, the contacts are modeled by normal contact forces and friction forces. Contact algorithm is presented to simulate the interaction between the feet and the ground or the knee locking mechanism as well. The foot can be considered as a special sphere for the compass-like walker or a series of points for other models like flat foot while the ground is considered as a plane. Thus, a general sphere/point–plane contact scheme is adopted here to model their contacts, as shown in Fig. 2 (a) and (b).

The contact force vector $\mathbf{F}$ contains a normal force and a friction force, $\mathbf{F} = F_n\mathbf{n} + F_\tau\boldsymbol{\tau}$, $\mathbf{n}$ is the unit normal direction of the contact point, $\boldsymbol{\tau}$ is the relative slip direction. The normal contact force F_n is given by Hunt–Crossley contact model,[21]

$$F_n = \max\left(k_c\delta^n + c_c\delta^n\dot{\delta}, 0\right) \tag{2}$$

where δ is the normal penetration depth. If $\delta < 0$, there is no contact interaction and the contact force is zero. $\dot{\delta}$ is the normal penetration velocity, k_c is the normal stiffness, c_c is the normal damping ratio and $n = 1.5$. If F_n is negative, then it will be set as zero.

Coulomb law is used for frictional force, $F_\tau = \mu\,(v_t)\,F_n$, where v_t is the relative slip velocity magnitude, and $\mu(v_t)$ is the coefficient of friction.[22] To avoid singularity, $\mu(v_t)$ is defined as

$$\begin{aligned}
\mu\,(v_t) &= \begin{cases} step(v_t, v_s, -\mu_s, v_d, -\mu_d) & v_s \le v_t \\ step(v_t, -v_s, \mu_s, v_s, -\mu_s) & 0 \le v_t < v_s \end{cases} \\
step\,(x, x_0, y_0, x_1, y_1) &= \begin{cases} y_0 & x \le x_0 \\ y_0 + a\Delta^2\,(3 - 2\Delta) & x_0 < x < x_1 \\ y_1 & x \ge x_1 \end{cases}
\end{aligned} \tag{3}$$

as shown in Fig. 2(c), where $a = y_1 - y_0$, $\Delta = (x - x_0)\,/\,(x_1 - x_0)$.

2.3. Modeling of event-based operating strategies

An event refers to a moment of concern that happens during walking, such as heel strike, toe-off and so on. Traditional impact-based method requires event-based switching of control equations and system state at the moment of foot strike impact with the ground. Though the presented framework, which uses force-based method, need not to handle these switchings, it is still necessary to monitor walking status and to know when to implement control or actuation, such as foot clearance, knee locking and so on during the solving process. All of such processes are based on events and thus referred to as event-based operating strategies for unified modeling, the schematic of which is shown in Fig. 3. The strategies are implemented at each integration step, where inputs are a series of predefined values as a function of current system state and outputs are a series of control variables.

The second PDW walker with flat feet and compliant ankles is used as an example to illustrate the modeling of event-based operating strategies in detail. The inputs include $\{F_n^R, F_n^L, \theta_h, x_{\text{hip}}, y_{\text{rheel}}, y_{\text{rtoe}}, y_{\text{lheel}}, y_{\text{ltoe}}\}$, which are normal contact force of right foot, normal contact force of left foot,

https://doi.org/10.1017/S0263574719000274 Published online by Cambridge University Press

Table I. Definitions of events for the PDW walker with flat feet and compliant ankles.

No.	Event name	Meaning	Conditional formula
1	Left foot-on	Left foot touches the ground	$F_n^L(\mathbf{q}) > 0$
2	Right foot-on	Right foot touches the ground	$F_n^R(\mathbf{q}) > 0$
3	Left foot-off	Left foot leaves the ground	$F_n^L(\mathbf{q}) = 0$
4	Right foot-off	Right foot leaves the ground	$F_n^R(\mathbf{q}) = 0$
5	Left foot-above	Left foot swings above the ground	$y_{\text{lheel}}(\mathbf{q}) > 0$, $y_{\text{ltoe}}(\mathbf{q}) > 0$
		Left leg swings past right leg	$\theta_h(\mathbf{q}) < 0$
6	Right foot-above	Right foot swings above the ground	$y_{\text{rheel}}(\mathbf{q}) > 0$, $y_{\text{rtoe}}(\mathbf{q}) > 0$
		Right leg swings past left leg	$\theta_h(\mathbf{q}) > 0$

Fig. 3. Schematic of event-based operating strategies.

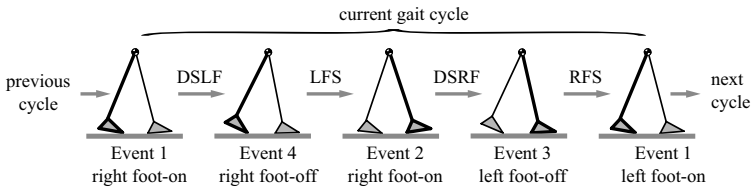

Fig. 4. Schematic of key events and phases for the PDW walker with flat feet and compliant ankles (the right leg is in bold).

relative angle between two legs, x-axis position of hip, relative y-axis position of heel and toe of two feet to the ground, respectively. Based on these inputs, the events listed in Table I are detected for operating strategies during the solution. The function of the events are calculated at each integration step. An event is triggered once the value of its conditional formula changes from False to True.

The events can be used to monitor walking status, which is used to know whether the walking is periodic and to obtain the gait parameters. For instance, a gait cycle is divided into four phases by whether the walker is single-foot support or double-feet support after the foot strike or toe-off. These four phases are named as double-feet-support-to-left-foot-support (DSLF) phase, left-foot-support (LFS) phase, double-feet-support-to-right-foot-(DSRF) phase and right-foot-support (RFS) phase, and are determined by the events as shown in Fig. 4.

The outputs are used for special control or actuation. Take the foot clearance as an example, the outputs include $\{\text{valid}_c^R, \text{valid}_c^L\}$, which are switches for contact detection between the right foot and the ground and for contact detection between the left foot and the ground, respectively. The value of valid_c^R is set to be False after event of right foot-off to turn off the contact detection, and set to be True after event of right foot above the ground to turn on the contact detection. Similar strategies are done for valid_c^L.

In addition, gait failure detection and gait parameter statistics are also needed to carry out. For example, a gait is viewed as failed if it fails to switch from one phase to the next one within a given duration. Gait parameters, that is, step length, step period and average speed, are calculated once a whole step is completed, and are used for further searching of periodic gaits and termination of the calculation.

3. Stable Periodic Gait Searching Algorithm and Stability Analysis

The governing equations (1) in the standard form of multibody dynamics system are a set of differential algebraic equations (DAEs), which can be numerically solved through the backward differentiation formula.[23] However, the DOFs are relatively large and the initial conditions are highly dimensional as a byproduct of the force-based method, leading to that it is difficult to find a stable

https://doi.org/10.1017/S0263574719000274 Published online by Cambridge University Press

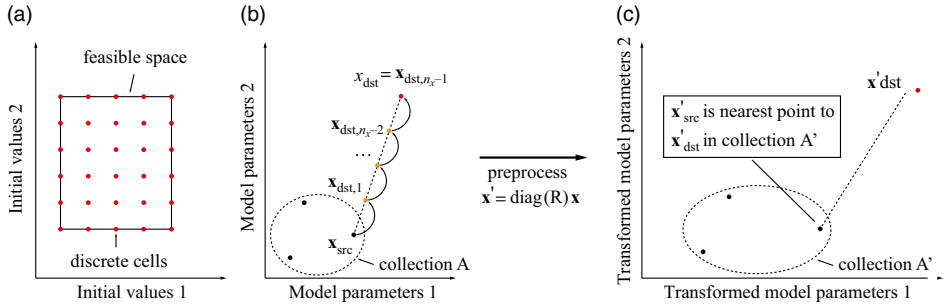

Fig. 5. Schematic of two-step stable periodic gait searching algorithm. (a) Cell discretization in the space of initial values to find a stable periodic gait. (b) and (c) Stable periodic gait searching method with the existing stable periodic gaits in the space of model parameters.

periodic gait. This section presents a fast and efficient algorithm to find a stable periodic gait for any given LCW model. Then, a stability analysis that could be easily implemented in the proposed framework is presented in detail. Besides, in the following of this section, the second PDW walker with flat feet and compliant ankles is taken as an example to illustrate the process clearly.

3.1. A fast and efficient algorithm for searching a stable periodic gait

By using Poincaré mapping method, the periodic gait corresponds to a fixed point on Poincaré section. The main idea is as follows. Let $\mathbf{p} = \left[p_1, p_2, \ldots, p_{n_p}\right]^{\mathrm{T}}$ be a set of generalized parameters of the walking model. A step function maps a point to another one on the Poincaré section:

$$\mathbf{v}_{n+1} = \mathbf{S}(\mathbf{v}_n) \tag{4}$$

where $\mathbf{v} = \left[\mathbf{p}^{\mathrm{T}}\ \dot{\mathbf{p}}^{\mathrm{T}}\right]^{\mathrm{T}}$ is the system state vector. To get a periodic gait is to get $\mathbf{v}^*$ that satisfies $\mathbf{v}^* = \mathbf{S}(\mathbf{v}^*)$. By given a initial value vector $\mathbf{v}_0$, Eq. (4) can be iteratively solved until $||\mathbf{v}_{n+1} - \mathbf{v}_n|| < \boldsymbol{\epsilon}$ is satisfied. In practice, the gait parameters, that is, step length, step period and average speed, are calculated after a gait cycle of four phases is finished. The gait is regarded as periodic as long as the standard deviation of the average speed of the last N_c steps is less than a given error ϵ_c. In this study, $N_c = 5$, $\epsilon_c = 5 \times 10^{-5}$. By the way, the periodic gait that is found is stable because this periodic gait is converged from a initial value and it can walk persistently and does not fall, which is the definition of walking stability.

However, the initial value $\mathbf{v}_0$ is very important as improper initial value will not lead to fixed points. To get a proper initial value, a simple idea is using cell mapping method[6,24] by testing all possible combination of system state. However, this would need a lot of computations for high-dimensional system state of the force-based method. As an example, the second PDW walker has six DOFs, so the dimension of its system state is 12. To the best of our knowledge, it still needs efficient ways to obtain a proper initial value of such a high-dimensional system state. Recently, Gan propagates one periodic solution to the others by solving a one-dimensional continuation problem and studies different gaits of a single passive walking model.[25] Here, a two-step searching algorithm for the initial value $\mathbf{v}_0$ is proposed to obtain the stable periodic gait for any given models. The second PDW walker is taken as an example to illustrate the implementation of the algorithm.

In the first step, the dimension of the initial value is minimized from 12 to 5, greatly decreasing computation cost. The initial state of the walker is set at the start of DSLF phase (the Event 1 of left foot-on), and then it is assumed that the contact normal force between right foot and the ground is equivalent to the weight of the walker by setting its penetration depth as a given value, left ankle is at its equilibrium position and angular velocities of left foot and left leg are the same. In this way, the initial values are reduced to five variables, that is, angle between right foot and right leg, angle between two legs, angular velocity of right foot, angular velocity of right leg and angular velocity of left leg. Feasible ranges are then selected for these variables to create the searching space that is further discretized into finite cells, represented by check points. All these cells are used as the initial system state to test whether they can lead to stable periodic gaits. The searching process could be stopped once a stable periodic gait is obtained. Figure 5(a) gives a simple schematic of

https://doi.org/10.1017/S0263574719000274 Published online by Cambridge University Press

cell discretization of a two-dimensional space. Therefore, at least one stable periodic gait has been obtained under a certain set of model parameters in this first step.

In the second step, the searching of a stable periodic gait of other sets of model parameters could be speeded up with the help of the known stable periodic gaits obtained in the first step. For clarity, Fig. 5(b) and (c) shows a simple schematic of this step in a two-dimensional space of model parameters. The main idea uses system state of the known stable periodic gait as initial value to iteratively obtain the new stable periodic gait of other different set of model parameters. It is based on an assumption that the stable periodic gait of the new model could be obtained by using the system state of the old model as the initial condition, which is reasonable if the variation of the two sets of model parameters is small. Let $\mathbf{x} = \left[\gamma\ k_h\ k_a\ k_c\ c_c\ \mu_s\right]^{\mathrm{T}}$ be the variable vector of model parameters of the second PDW walker since its mass and geometrical parameters are fixed. Naming that the model variable that needs to seek stable periodic gait is $\mathbf{x}_{\mathrm{dst}}$ and the collection $\mathbf{A}$ is a list of vector $\mathbf{x}$ whose periodic gaits have already been gained. As the periodic gait has different sensitivity to different model variables, a transformation is done for $\mathbf{x}_{\mathrm{dst}}$ and items $\mathbf{x}$ in $\mathbf{A}$, $\mathbf{x}' = \mathrm{diag}\,(\mathbf{R})\,\mathbf{x}$. The vector $\mathbf{R}$ represents the sensitivities of periodic gaits to model parameters. If the periodic gait is greatly affected by a model parameter, then the corresponding value in $\mathbf{R}$ should be large. From the perspective of accuracy, it is better to select larger values for $\mathbf{R}$. However, this would slow down computational efficiency. In practice, each value in $\mathbf{R}$ is selected manually by testing whether it is efficient for periodic gait searching when changing corresponding model parameter only. For the PDW walker with flat feet and compliant ankles, $\mathbf{R}$ is selected as

$$\mathbf{R} = \left[20\ 0.2\ 0.1\ 10^{-5}\ 5 \times 10^{-6}\ 20\right] \tag{5}$$

In the transformed space, the point $\mathbf{x}'_{\mathrm{src}}$ in $\mathbf{x}'$ of the collection $\mathbf{A}$ has a minimum distance to $\mathbf{x}'_{\mathrm{dst}}$. If $\left\|\mathbf{x}'_{\mathrm{dst}} - \mathbf{x}'_{\mathrm{src}}\right\| \leq 1$, then the system state at the start of DSLF phase of the stable periodic gait of $\mathbf{x}_{\mathrm{src}}$ is used to obtain the new stable periodic gait. If $\left\|\mathbf{x}'_{\mathrm{dst}} - \mathbf{x}'_{\mathrm{src}}\right\| > 1$, then $n_x = \mathrm{ceil}\left(\left\|\mathbf{x}'_{\mathrm{dst}} - \mathbf{x}'_{\mathrm{src}}\right\|\right) + 1$ points are defined:

$$\mathbf{x}_{\mathrm{dst},i} = \mathbf{x}_{\mathrm{src}} + \frac{i}{n_x - 1}\left(\mathbf{x}_{\mathrm{dst}} - \mathbf{x}_{\mathrm{src}}\right),\ i = 0, 1, 2, \ldots, n_x - 1 \tag{6}$$

Starting from $i = 1$, stable periodic gait of $\mathbf{x}_{\mathrm{dst},i}$ is obtained using the system state of the stable periodic gait of $\mathbf{x}_{\mathrm{dst},i-1}$ as the initial value until the stable periodic gait of $\mathbf{x}_{\mathrm{dst},n_x-1}$ is obtained. If this strategy fails to find a stable periodic gait, it is then considered that there is no stable periodic solution under the given set of model parameters.

The two-step searching algorithm for stable periodic gait can be summarized as the following. First, the dimension of initial values is reduced as much as possible to cut computation cost by setting the walker at the start of DSLF phase, and then cell mapping method is used to obtain stable periodic gait under a certain set of model parameters. The second step is to obtain the stable periodic gait of arbitrary model parameters by using system state of known stable periodic gait as initial value, decreasing computation cost further.

It is noteworthy that this algorithm is suitable for those regions in the space of model parameters that stable periodic gait exists are connected. For non-connected cases, this method should be extended by trying different initial values to test non-connected areas. By the way, the BoA could be easily implemented by using this algorithm.

3.2. Stability analysis

For LCW, there are a number of stability indicators, such as maximum Floquet multipliers, the BoA,[6] Gait sensitivity norms,[14] maximum allowable disturbance,[1] among which the maximum allowable disturbance is an important index for robustness.[26] The maximum allowable disturbance applies a maximum real-world disturbance, such as ground irregularity, slope irregularity or sudden pushes that the walker can tolerate as the index. In this study, the maximum allowable disturbance that includes maximum allowable step-down height and step-up height is used instead. For this method, a foot of the walker is assumed to step through a step whose height is h_s. The maximum h_s and minimum h_s that the walker can tolerate are calculated. Figure 6 gives the schematic of stability test.

https://doi.org/10.1017/S0263574719000274 Published online by Cambridge University Press

Table II. Parameters of the compass-like PDW walker.

Item	**Symbol and value**
Leg length	$l = 0.4143$ m
Radius of foot	$\rho = 0.0860$ m
Slope	$\gamma = 2.05$ degree
Leg mass	$m = 5.1587$ kg
Lumped mass	$M = 1.2826$ kg
Mass center of leg	$b = 0.1930$ m
Radius of gyration	$r_g = 0.1067$ m
Contact stiffness	$k_c = 9.3920 \times 10^5$ kg m$^{-1/2}$s^{-2}
Contact damping	$c_c = 1.6879 \times 10^7$ kg m$^{-3/2}$s^{-1}
Friction parameters	$v_s = 0.01$ m/s, $v_d = 0.02$ m/s
Friction coefficient	$\mu_s = 0.5$, $\mu_d = 0.4$

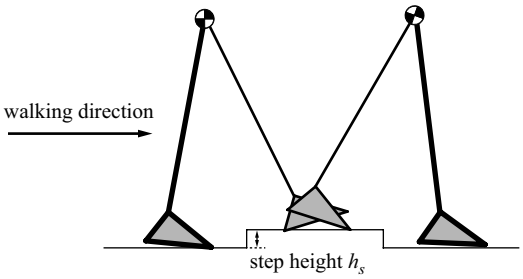

Fig. 6. Schematic of the walker walking through a step with a height of h_s.

$h_s > 0$ means that the step is above the ground. The step position and width are carefully set to let just one foot step through it. This method could be easily implemented in the proposed framework.

4. Verification and Application Examples

4.1. Example 1: verification with a compass-like PDW walker

The model of Koop[3] is used as a verification example. As shown in Fig. 1(a), the model consists of two legs and a lumped mass. The two legs are revolutely joined together at their up ends to represent the hip joint, and the lumped mass is attached to one of the leg at the revolute joint to simplify the upper body. The contact between the foot and the ground is modeled as contacts between a sphere and a plane. The values of model parameters are listed in Table II, which are the same as those of Koop's[3] for comparing the results.

The control strategy of this model is similar to that of the PDW walker with flat feet and compliant ankles, which is adopted to deal with the ground clearance. To achieve good accuracy and to shorten the calculation time, the max error of the integrator is set as 10^{-5}, and the max step is 1×10^{-4} s.

The stable periodic gait of this model is obtained by the presented method. The results are compared with those of Koop as shown in Fig. 7. The curve of phase trajectory of the leg, the curves of the angle of the leg and the normal contact force are all in full agreement with the results of Koop. For the friction force, the curve of this study is consistent with that of Koop, but there is a difference of two spike values at the two moments of heel strike and toe-off where the results of Koop are larger than this study. This difference in spike may result from different friction model and actually has no influence on the walking results. In addition, the spike is usually better to be smaller, so the Coulomb friction model adopted here is accurate and its form is simpler than LuGre friction model used by Koop. For the simulation video of this stable periodic gait, please see Example1.avi in the Supplementary Material.

Several models with the same sets of model parameters as the Koop's models have been simulated, and the corresponding stable periodic gaits are obtained. The group of the parameters are listed in

https://doi.org/10.1017/S0263574719000274 Published online by Cambridge University Press

Table III. Parameters of different cases for the compass-like PDW walker.

Case index	**Mass center b (m)**	**Radius of gyration r_g (m)**
1	0.1356	0.1192
2	0.1547	0.1112
3	0.1739	0.1077
4	0.1930	0.1067
5	0.2122	0.1091
6	0.2313	0.1146

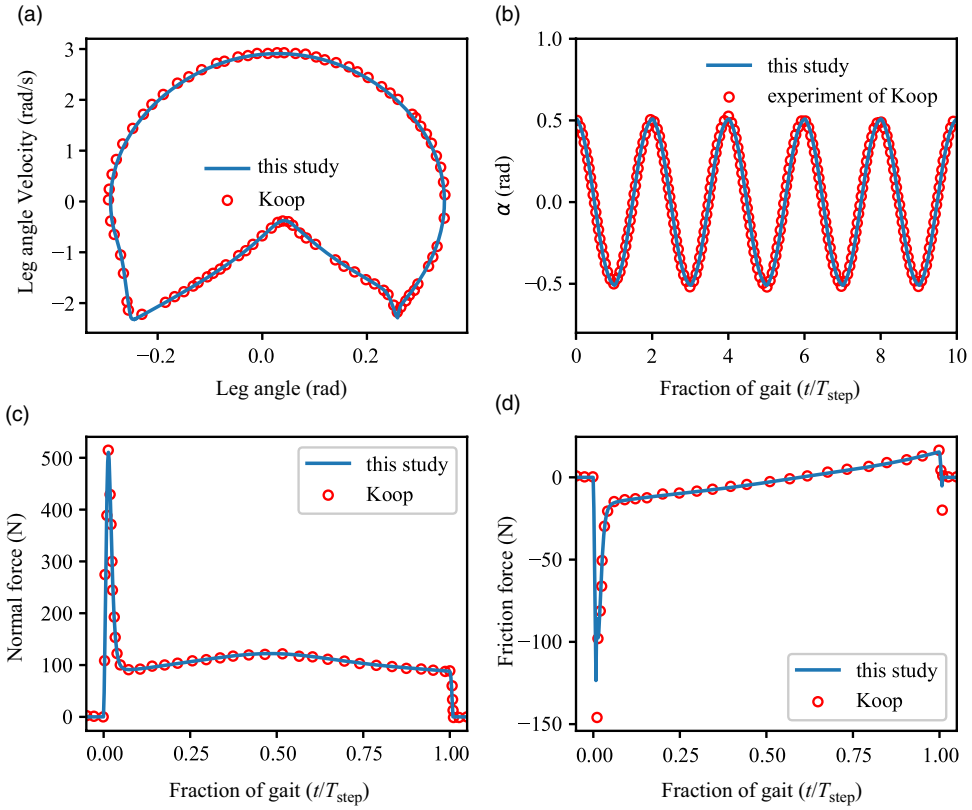

Fig. 7. Comparison of results of stable periodic gait with Koop. (a) Phase trajectory of one leg, (b) leg angle versus the time, (c) ground reaction normal force versus the time and (d) ground reaction friction force versus the time.

Table III. The step period and the average speed are compared with those of Koop, as shown in Fig. 8, which are in good agreement. In conclusion, the results of our simulations agree well with the experimental and simulational results of Koop, verifying the correctness of the proposed solution.

4.2. Example 2: a PDW walker with flat feet and compliant ankles

This section presents a PDW walker with flat feet and compliant ankles. Similar walkers have been investigated in the literature.[9,10,27] Compared with point foot, flat foot has higher efficiency.[7] And compared with arc foot, flat foot can realize standing, just like human. Conclusions have been drawn that the ankle and the ankle spring further increase the walking efficiency, and proper ankle spring stiffness is very important to the walking efficiency.[9,27] Theoretically, zero energy cost could even be achieved with proper parameters as stated in ref. [9]. This example reanalyzes this model to verify the correctness of the presented framework by comparing results with those of the previous researches. Besides, all of the previous researches are based on the conventional impact-based method, so the comparison can reveal the advantage of the proposed solution.

https://doi.org/10.1017/S0263574719000274 Published online by Cambridge University Press

Table IV. Properties of geometry, mass, mass center and inertia of Example 2.

Item	**Symbol and value**
Leg length	$l_l = 0.8276$ m
Foot length	$l_f = 0.18$ m
Foot height	$h_f = 0.05$ m
Leg mass	$m_l = 13.0089$ kg
Foot mass	$m_f = 1.5666$ kg
Lumped mass	$m_a = 46.0136$ kg
Mass center of leg	$c_l = 0.2881$ m
Mass center of foot	Center of triangle
Inertia of leg	$J_l = 0.6473$ kg m^2
Inertia of foot	$J_l = 0.0082$ kg m^2

Table V. Spring parameters of Example 2.

Item	**Symbol and value**
Ankle spring stiffness	k_a, to optimize
Ankle spring damping	$c_a = \sqrt{J_{fa} k_a}$
Ankle spring equilibrium position	$\theta_{a0} = 95°$
Hip spring stiffness	k_h, to optimize

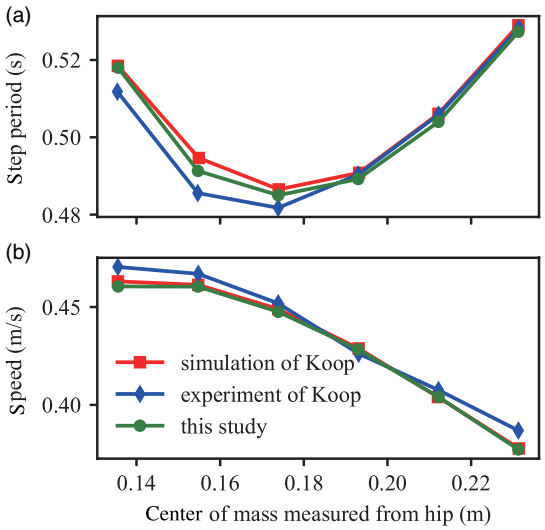

Fig. 8. Comparison of general information with Koop's results for several different cases. (a) Step period and (b) speed.

The parameters of this model are extracted from the Gait2392 model[28] of OpenSim.[29] The body height is 1.8 m and the weight is 75.16 kg, with other parameters listed in Table IV. The lumped mass represents the weight of the upper part of the body and is revolutely joined to the upper end of one leg. Schematic of a foot is shown in Fig. 1(d). The relative length of heel is $r_f = 0.25$. The parameters of the torsional springs are listed in Table V. The damping of ankle spring is $\sqrt{J_{fa} k_a}$, which is half of the critical damping, where J_{fa} is the rotational inertia of the foot to the heel joint. Simulation tests show that this value could quickly suppress oscillation between the swing leg and the corresponding foot. The contact between the flat foot and the ground is modeled by contacts of the heel point and the toe point with a plane. Thus, there are four pairs of contacts: contact 1 is between the right heel and the ground; contact 2 is between the right toe and the ground; contact 3 is between the left heel

https://doi.org/10.1017/S0263574719000274 Published online by Cambridge University Press

Table VI. Contact parameters of example 2.

Item	Symbol and value
Contact stiffness	$k_c = 1 \times 10^6\ \mathrm{kg\,m^{-1/2}s^{-2}}$
Contact damping	$c_c = 5 \times 10^6\ \mathrm{kg\,m^{-3/2}s^{-1}}$
Friction parameters	$v_s = 0.01$ m/s, $v_d = 0.02$ m/s
Friction coefficient	$\mu_s = 0.5$, $\mu_d = 0.4$

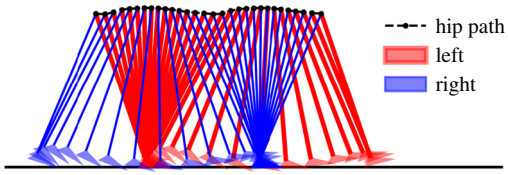

Fig. 9. Stick figure of the typical stable periodic gait of the PDW walker with flat feet and compliant ankles.

and the ground; contact 4 is between the left toe and the ground. And other contact parameters are listed in Table VI.

4.2.1. Typical stable periodic gait like human. A set of model parameters of PDW may have a unique stable periodic gait, which could be solved by the searching method presented in Section 3.1. In this section, a typical stable periodic gait whose gait parameters are similar to human[30] is expected by optimizing the variable model parameters. The object step length is $l^0_{\mathrm{step}} = 1.25$ m and the step period is $T^0_{\mathrm{step}} = 1$ s, and it also has a minimum energy cost. Specially, the optimization space is $\mathbf{A} = \left\{\mathbf{x} | \mathbf{x} \in \mathbb{R}^3\right\}$, $\mathbf{x} = (\gamma, k_a, k_h)$ and the object function fmin : $\mathbf{A} \to \mathbb{R}$ is

$$\mathrm{fmin}\,(\mathbf{x}) = \left(l_{\mathrm{step}} - l^0_{\mathrm{step}}\right)^2 + \left(T_{\mathrm{step}} - T^0_{\mathrm{step}}\right)^2 + w_\gamma \gamma \tag{7}$$

where l_{step} and T_{step} are, respectively, the step length and period of the stable periodic gait under given optimal vector, $w_\gamma = 10^{-4}$ is the optimal weight of slope angle and the unit of γ is degree. First the presented algorithm in Section 3.1 is applied to obtain the stable periodic gait for initial set of model parameters, then the simplex optimization method[31,32] is adopted to optimize the model parameters to get the human-like gait. If it fails to obtain a periodic gait, the object function value is set to a higher value, 100 in this case.

The model parameters of the optimized typical stable periodic gait are $k_h = 109.15\ \mathrm{N\,m\,rad^{-1}}$, $k_a = 364.73\ \mathrm{N\,m\,rad^{-1}}$ and $\gamma = 1.567^\circ$ (≈ 0.027 rad). And correspondingly, the walking speed is 1.249 m/s, the step period is 1.0 s and the step length is 1.248 m. During the solving process, this model is assumed to begin at the DSLF phase. The initial values include five parts, namely, angular velocity of right foot ω_{rfoot0}, angular velocity of right leg ω_{rleg0}, angular velocity of left leg ω_{lleg0}, angle between legs θ_{h0} and left ankle angle $\theta_{\mathrm{rankle0}}$. The feasible space range and subdivided count for the initial values can be set as follows: $\omega_{\mathrm{rfoot0}} \in [-4.5, -0.5]$ and $N = 8$, $\omega_{\mathrm{rleg0}} \in [-4.5, -0.5]$ and $N = 8$, $\omega_{\mathrm{lleg0}} \in [-4.5, -0.5]$ and $N = 8$, $\theta_{h0} \in [1/6\pi, 1/4\pi]$ and $N = 5$, and $\theta_{\mathrm{rankle0}}$ is fixed to 85 degree. There are 2560 cells in total and 374 cells are able to lead to a stable periodic gait.

Walking gait

The typical stable periodic gait is shown in Fig. 9. The curves of the hip angle, ankle angle and ground reaction force are shown in Fig. 10. The walking sequence of a typical stable periodic gait is given as follows. First, the body is at the state of double-feet supporting and the right leg is the leading leg. At this moment, the right heel has just contacted with the ground, while the left heel has left the ground and the left ankle is in compression. Then, as the body moves forward, the compression of the left ankle decreases until the left toe leaves the ground and starts to swing forward, entering into right-foot-support phase. After that, the right toe touches the ground and right foot full flats on the ground and then right heel leaves the ground. After the left heel contacts with the ground again, the

https://doi.org/10.1017/S0263574719000274 Published online by Cambridge University Press

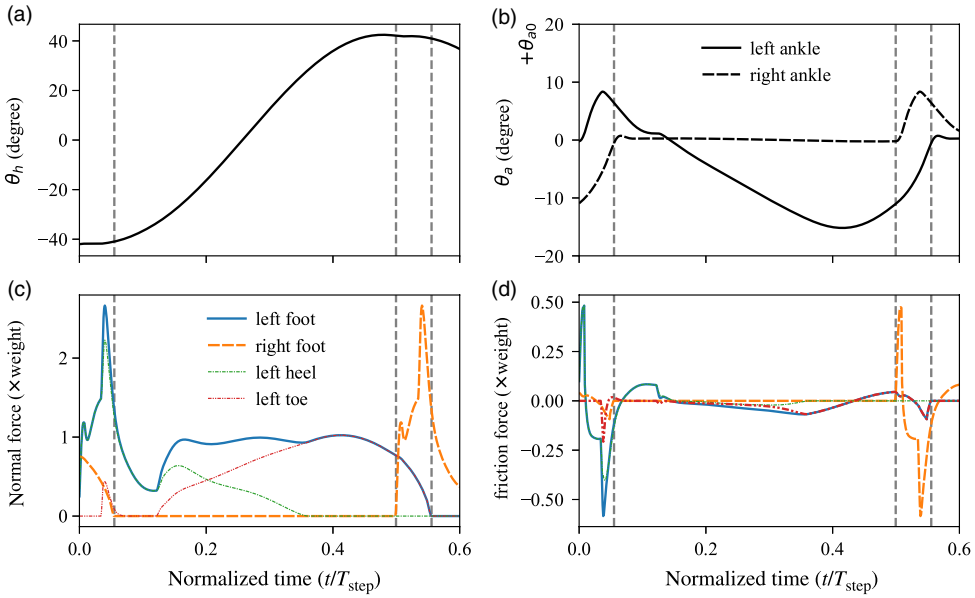

Fig. 10. Curves of (a) hip angle, (b) ankle angle, (c) ground reaction normal force and (d) ground reaction friction force versus normalized time.

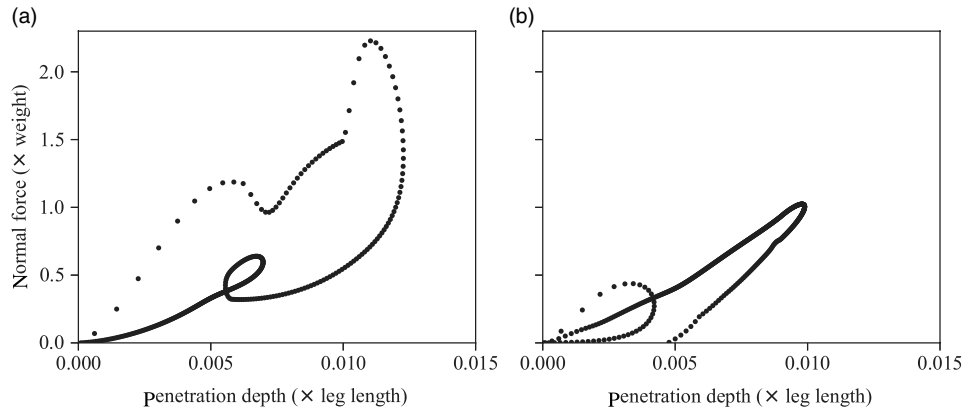

Fig. 11. Ground reaction normal force as a function of penetration depth for (a) heel–ground contact and (b) toe–ground contact.

next double-feet-support phase begins while the leading leg is the left leg, and the process is similar as the body moves on. For the simulation video of this stable periodic gait, please see Example2.avi in the supplemental material.

During a gait cycle, the peak of friction force occurs at the double-feet-support phase as shown in Fig. 10. At the moment of the leading foot contacting with the ground, the friction force is positive, and then it changes direction to be negative. The maximum friction force is about half of the body weight. The duration of double-feet-support phase is 11% of the walking cycle, less than 20% of a typical human.

During the double-feet-support phase, the toe of the leading leg bounces after its first contact with the ground, and then comes to a second contact to realize foot-flat. This phenomenon has not been described in the available literature. It means that the walking perhaps is very complicated and man-made walking gait may be obtained when using conventional hybrid system to analyze this complex model. And the multibody method does not need any assumption of the walking gait and may obtain a more realistic gait. The reasons of phenomenon and how to avoid it are not the focus of this paper.

The curves of the normal contact force versus the penetration depth of the heel–ground contact and toe–ground contact are given in Fig. 11. The relation of normal contact force with the penetration is given by Eq. (2). The maximal penetration depth of the heel is about 1.2% of the leg length.

https://doi.org/10.1017/S0263574719000274 Published online by Cambridge University Press

Energy cost analysis

The energy dissipation is analyzed in this subsection in detail. During the walking process, four parts of energy are involved in the system: kinetic energy, gravitational potential energy, elastic potential energy (resulting from torsional spring at the hip point and at the ankle) and the stored energy when contacting with the ground. In the walking process, these four parts of energy convert among them and there also exists energy dissipation. When the walking is periodic, the kinetic energy, the potential energy and the storing energy does not change at the start and the end of a step. And the decrease of the gravity potential energy is the total energy dissipation.

The walking efficiency is defined by mechanical energy cost of transport (mCOT).[33] For a walker walking a constant slope γ, mCOT equals $\sin\gamma$. Therefore, the mCOT of the typical stable periodic gait is 0.027 and the energy loss in a step is $E_{\text{total}} = -25.18$ J.

The energy loss includes three parts: the negative work caused by the two damping of the ankle springs , by the contact damping of the four pairs of contacts and by the friction forces of the four pairs of contacts, denoted as E_a, E_{cy} and E_{cx}, respectively.

The power rate of ankle spring damping is

$$P_a^i(t) = -c_a \cdot \left(\omega_l^i(t) - \omega_f^i(t)\right)^2 \tag{8}$$

where $\omega_l^i(t)$ and $\omega_f^i(t)$ are angular velocity of leg and foot, respectively. Superscript $i = 1$ or 2, representing left ankle and right ankle, respectively.

For the ith pair of contact, the power rate of contact damping is

$$P_{cy}^i(t) = \begin{cases} -c_c\delta_i(t)^{\frac{3}{2}}\dot{\delta}_i(t)^2 & F_n^i(t) > 0 \\ -k_c\delta_i(t)^{\frac{3}{2}}\dot{\delta}_i(t) & F_n^i(t) = 0 \text{ and } \delta_i(t) > 0 \text{ and contact is valid} \\ 0 & \text{others} \end{cases} \tag{9}$$

where $\delta_i(t)$ is the penetration depth, $\dot{\delta}_i(t)$ the velocity of penetration depth and $F_n^i(t)$ the contact normal force.

The power rate of the friction force is

$$P_{cx}^i(t) = -\left|F_\tau^i(t)\, v_\tau^i(t)\right| \tag{10}$$

where $F_\tau^i(t)$ is the contact friction force, $v_\tau^i(t)$ the tangential velocity.

For a power function, cumulative energy loss is defined as

$$E(f,t) = \int_{t_0}^{t} f(t)dt, \quad t \in \left[t_0, t_0 + T_{\text{step}}\right] \tag{11}$$

where $f(t)$ is the power rate function, t_0 is the time at the start of periodic gait and T_{step} is the step period.

Figure 12 shows the energy loss of different sources within a gait cycle. During one-step cycle, the heel-related contact damping loses 44.6% of total energy dissipation, the ankle spring damping loses 34.4% of total energy dissipation, the toe-related contact damping loses 15.5% of total energy dissipation and the contact friction force loses the final 5.5% of total energy dissipation. It can also be seen from Fig. 12, about 69.1% of the energy dissipation happens during double-feet-supporting phases. In addition, the energy efficiency of different model parameters and related periodic gaits under different speeds are obtained, and the results are combined with Example 3 and presented in Section 4.3.

4.2.2. Effect of contact parameters on walking efficiency and stability. In this subsection, the effects of contact parameters on walking efficiency and stability, which are two of the most important indicators for PDW, are studied. The variable parameters for contact are k_c and c_c, and the variable parameter that represents the friction is the friction coefficient μ_s, while it is assumed that $\mu_d = \mu_s - 0.1$ and both v_s and v_d are kept constant. A range of different k_c, c_c and μ_s is adopted to study their influence on walking efficiency and stability. Because the comparison of the efficiency and stability makes sense based on the same gait, the other model parameters γ, k_a, k_h are also changed with the varying k_c, c_c and μ_s to achieve the same gait. The walking efficiency can be indicated by

https://doi.org/10.1017/S0263574719000274 Published online by Cambridge University Press

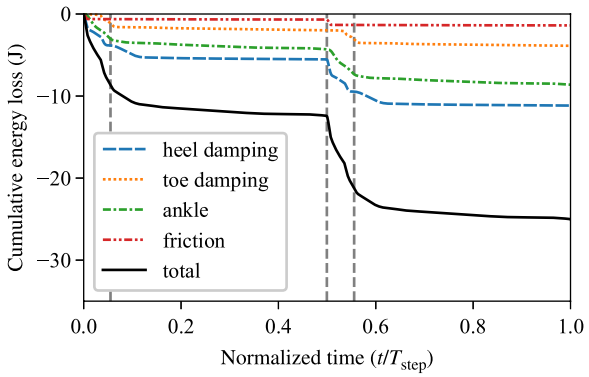

Fig. 12. Cumulative energy loss of different energy dissipation sources including these caused by heel-related contact damping (heel-damping), these caused by toe-related damping (toe-damping), ankle spring damping (ankle) and friction force (friction) within one step.

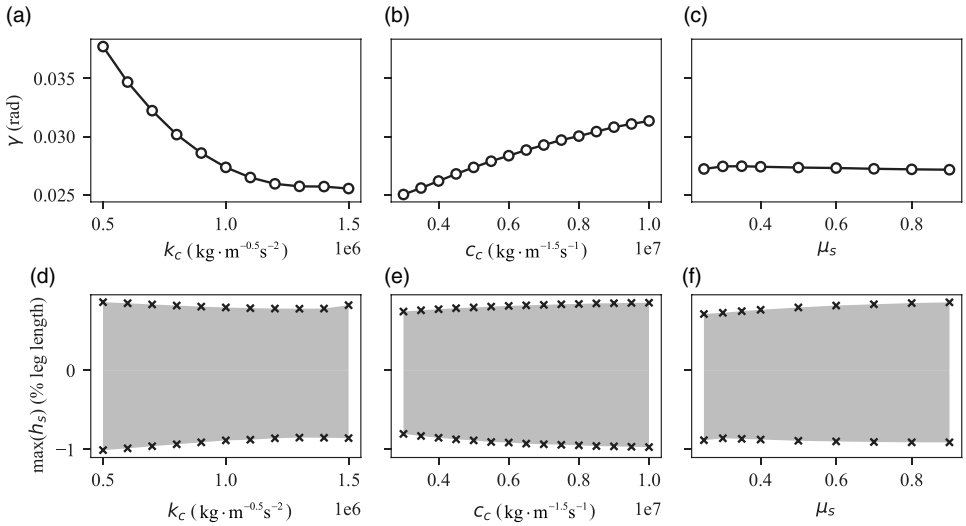

Fig. 13. Effect of contact stiffness, contact damping and friction coefficient on (a–c) walking efficiency and (d) and (e) maximum allowable disturbance. Object gait parameters are kept constant, that is, $l^0_{\text{step}} = 1.25$ m and $T^0_{\text{step}} = 1$ s.

the slope angle as the dissipation energy is equal to the gravity potential energy, and the maximum allowable disturbances are used to indicate the global stability.

As shown in Fig. 13, the results demonstrate that both contact stiffness and contact damping have relatively large influence on walking efficiency. When the contact stiffness increases from 5×10^5 to 1.5×10^6 kg m$^{-1/2}$s^{-2}, the slope angle decrease from 0.038 to 0.026 rad which is 68%. Furthermore, when the stiffness is larger than 1.5×10^6 kg m$^{-1/2}$s^{-2}, its influence on the efficiency is limited as the gradient is almost zero. And when contact damping increases from 3×10^6 to 1×10^7 kg m$^{-3/2}$s^{-1}, the slope angle increases from 0.025 to 0.031 rad. The influence of contact damping can be interpreted by the mentioned energy cost analysis, that is, large damping rate means large dissipation energy. By the way, there is little influence of the friction coefficient on energy efficient, but when μ_s is less than about 0.3, a stable periodic gait is failed to obtain because there is an evident foot slip. As a result, high contact stiffness and low contact damping benefit walking efficiency, but if the contact stiffness is larger than 1.5×10^6 kg m$^{-1/2}$s^{-2}, its influence is limited. These results are consistent with the results of a simple compass-like PDW by Qi et al.[12] that both high contact stiffness and low contact damping enable fast walking speed in the same slope, while friction parameters have few effect.

The global stability analysis show that the maximum step height disturbance is about 1% leg length no matter how these three parameters change, as shown in Fig. 13. That is to say, all the

https://doi.org/10.1017/S0263574719000274 Published online by Cambridge University Press

Table VII. Parameters of the level-walking walker.

Item	Symbol and value
Ankle actuation	$\tau_a = 30\,\text{N m}$
Hip actuation	$k_h = 25\,\text{N m/rad}$
Hip actuation	$\theta_{h0} = 0.16\,\text{rad}$
Ankle spring stiffness	$k_a = 360\,\text{N m/rad}$
Thigh length	$l_t = 0.3976\,\text{m}$
Shank length	$l_s = 0.43\,\text{m}$
Thigh mass	$m_t = 9.3014\,\text{kg}$
Shank mass	$m_s = 3.7075\,\text{kg}$
Thigh inertia	$J_t = 0.1412\,\text{kg m}^2$
Shank inertia	$J_s = 0.0511\,\text{kg m}^2$
Mass center of thigh	$c_t = 0.1700\,\text{m}$
Mass center of shank	$c_s = 0.1867\,\text{m}$
Knee lock parameters	$c_{k1} = 1000\,\text{N m}$
Knee lock parameters	$c_{k2} = 100\,\text{rad}^{-1}$

three parameters, k_c, c_c and μ_s, have little influence on stability. This is a good conclusion to choose the contact parameters. The conclusion may be drawn that only the periodic gait and the energy efficient should be considered to choose proper contact parameters, which could be easily verified by experimental tests.

4.3. Example 3: a level-walking walker with ankles and knees

A level-walking walker with ankles and knees as shown in Fig. 1(c) is discussed in this section. Compared to the PDW walker with flat feet and compliant ankles, this model has the following differences: (1) The leg is consisted of a thigh and a shank with a knee joint and the joint is fully passive. (2) This walker walks on the level ground by adding actuation at the ankle joint and hip joint. (3) The passive hip spring is omitted, since its function of adjusting walking frequency of PDW can be replaced by the control in this case. (4) A knee locking and unlocking strategy is introduced. (5) Strategy to implement ground clearance is omitted with the existence of knee joint.

The ankle actuation is introduced with a constant torque τ_a, which starts at when the ankle joint compresses most and stops just after the toe-off event. The hip torque is introduced to control leg swing. It starts just after double-feet-support phase and stops just after knee locking. The hip torque M_h is designed as a simple function of the leg angle

$$M_h\left(\theta_h\right) = \max\left(-k_h\left(\theta - \theta_{h0}\right), 0\right) \tag{12}$$

where k_h and θ_{h0} are both hip actuation parameters, θ the relative angle between swing leg to supporting leg.

The knee joint is restrained with a point–plane contact on one side, for which the impact-based method cannot be applied and only the force based is suitable. On the single support phase, a knee-locking torque is applied to the knee joint just after this point–plane contact occurs. To achieve a smooth impact, the knee-locking torque M_k is designed as

$$M_k = c_{k1} e^{-c_{k2}\theta_k} \tag{13}$$

where c_{k1} and c_{k2} are both constants, θ_k the angle of the knee joint.

Model parameters are listed in Table VII, and the other parameters are the same as the PDW walker with flat feet and compliant ankles.

To find its stable periodic gaits, this model begins at the DSLF phase. The initial values include five parts, namely, angular velocity of right foot ω_{rfoot0}, angular velocity of right leg ω_{rleg0}, angular velocity of left leg ω_{lleg0}, angle between legs θ_{h0} and left ankle angle θ_{rankle0}. The feasible space range and subdivided count for the initial values can be set as follows: $\omega_{\text{rfoot0}} \in [-4.5, -0.5]$ and $N = 8$, $\omega_{\text{rleg0}} \in [-4.5, -0.5]$ and $N = 8$, $\omega_{\text{lleg0}} \in [-4.5, -0.5]$ and $N = 8$, $\theta_{h0} \in [1/6\pi, 1/4\pi]$ and $N = 5$, and

https://doi.org/10.1017/S0263574719000274 Published online by Cambridge University Press

Table VIII. General information of the two stable periodic gaits of the level-walking model.

Information	**Gait 1**	**Gait2**
Speed (m/s)	1.002	0.755
Step length (m)	1.449	1.238
Step period (s)	1.447	1.639
mCOT	0.045	0.043
Double-feet-supporting phase (%)	8.1%	8.1%
Ankle work (%)	49.3%	53.4%
Hip work (%)	50.7%	46.6%
Ankle spring damping dissipation (%)	28.9%	23.8%
Foot contact dissipation (%)	20.7%	23.8%
Knee contact dissipation (%)	50.4%	52.4%

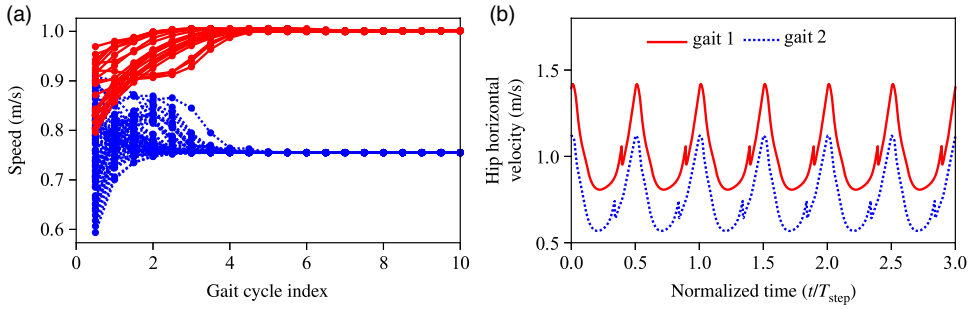

Fig. 14. (a) Convergence procedure of the level-walking model and (b) hip horizontal velocity versus normalized time for the two stable periodic gaits parameters.

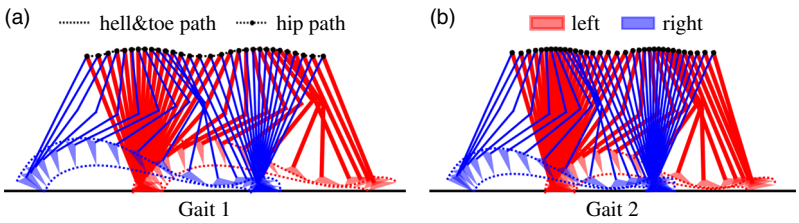

Fig. 15. Stick figure of two stable periodic gaits of the level-walking model.

θ_{rankle0} is fixed to 85 degree. There are 2560 cells in total and all of them are tested to verify whether it can lead to a stable periodic gait.

The simulations show that 89 cells are able to obtain a stable periodic gait. Figure 14(a) shows the average speed of the first 10 gait cycles of those cells. The speed is collected every half of gait cycle. Surprisingly, two distinct stable periodic gaits are obtained. The curves of hip horizontal velocities versus time of three gait cycles are shown in Fig. 14(b) for the two stable periodic gaits, the gait 1 of which has a much higher walking speed than the gait 2. Both gaits are natural looking, similar to the walking of human, as shown in the Fig. 15. For the simulation video of the high-speed stable periodic gait, please see Example3.avi in the supplementary material.

The general information of the two gaits is listed in Table VIII. Though their walking speed are different, their mCOTs are similar. Under the perspective of energy, the work imported by ankle actuation and hip actuation exactly compensate the energy dissipation during a gait cycle. Ankle actuation and hip actuation each provide about half of the work. By using similar energy cost analysis introduced in Example 2, about one-quarter of total input energy is dissipated in the ankle spring damping, one-quarter is dissipated in the foot contact, and the remaining half is dissipated in knee locking.

https://doi.org/10.1017/S0263574719000274 Published online by Cambridge University Press

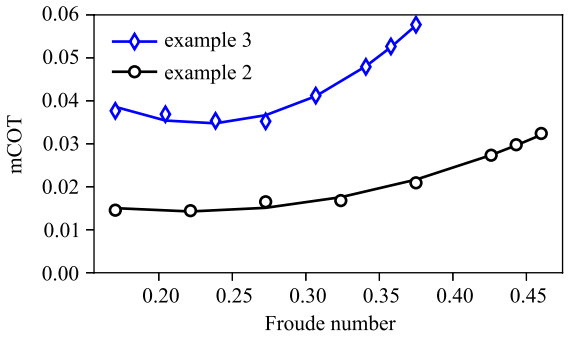

Fig. 16. Comparison of walking efficiency between Examples 3 and 2 under different Froude numbers.

Half of gait cycle is divided by six impact-related events, that is, left heel-on event, right toe-off event, left toe-on event, left toe-off event, left toe-on event and right knee-lock event. The sequence of these events is not unique, for example, left toe-on event may happen before right toe-off event. Thus, if traditional impact-based method is used, it requires six transitions of governing equations and system state. By the way, it may be impossible to model the knee-lock contact through the impact-based method. In addition, two points contacting a foot occupy part of gait cycle. In summary, such a complex model is difficult to analyze using impact-based method.

To compare the walking efficiency between Examples 2 and 3, different stable periodic gaits of different speeds are obtained under the corresponding model parameters with the relation between step length and walking speed being kept as $l_{\text{step}} \propto v^{0.42}$, which is similar to that of human.[34] In Example 2 the model parameters of k_h and k_a are changed, while in Example 3 τ_a and k_h are varied. For comparison, speed is non-dimensionalized by the Froude number

$$F_r = \frac{v}{\sqrt{gl}} \tag{14}$$

where l is the length of leg. mCOT of the periodic gaits of the two examples under different Froude number is shown in Fig. 16. The result of Example 2 indicates that mCOT increases as the Froude number increases, while in Example 3 mCOT decreases slightly and then rises quickly as the Froude number increases. The results further show that energy cost of Example 3 is more than twice of that of Example 2. As mentioned during the discussion of typical periodic gaits, this is mainly because almost half of energy is dissipated during the knee-locking process. It seems previous studies overlook the significant influence in walking efficiency of knee locking, while this study suggests efficient knee-locking mechanism and actuation strategies are in need to cut down walking cost a lot.

In conclusion, stable periodic gait of a level-walking model is obtained by adding a simple motion actuation. Interestingly, two stable periodic gaits are established for the completely same set of model parameters and actuation strategies. Detailed results show significant energy is lost by the knee locking, so this model is less efficient than the PDW walker with no knees. As an advantage, the presented method can be used to search for efficient leg swing and knee-locking strategies to improve walking efficiency remarkably.

5. Conclusion

This paper presents a general framework of numerical solution to the LCW based on multibody system dynamics, which could be used to study very complex models of the LCW. The governing equations of the system are established in a uniform manner as DAEs by using Lagrange equation of the first kind. Especially, the impact between the foot and the ground is modeled by force-based method and is presented in detail, which eliminates the discontinuity of the system state before and after the impacts based on impact-based method and also makes the system equation easy to be solved. The event-based operating strategies are proposed to realize model-related control strategies and to perform gait parameter statistics. Furthermore, a two-step searching algorithm is proposed to obtain stable periodic gait for any given complex model. Finally, a method for stability analysis is proposed, which could be easily implemented in this framework.

https://doi.org/10.1017/S0263574719000274 Published online by Cambridge University Press

Three examples are studied by using the proposed framework, respectively, a compass-like walker, a walker with flat feet and compliant ankles, and a level-walking walker with ankles and knees. The third model is hard to analyze with conventional method. Their stable periodic gaits are obtained respectively, and the results of the first two models agree well with those of the previous literature, verifying the correctness of the proposed method. Moreover, the results quantitatively illustrate the positive effect of ankle spring with proper spring stiffness on walking efficiency. The study of the third example, surprisingly, finds that there exist double stable periodic gaits for low and high walking speed, respectively, which have never been mentioned before. Therefore, the proposed framework is expected to assist in the analysis of complex walking models, optimization of model parameters and design of control strategies. Efficient actuation strategies and control strategies are going to be studied by this framework in the near future.

Supplementary Material

To view supplementary material for this article, please visit https://10.1017/S0263574719000274.

References

1. T. McGeer, "Passive dynamic walking," *Int. J. Rob. Res.* **9**(2), 62–82 (1990).
2. D. G. E. Hobbelen, *Limit Cycle Walking* (Delft University of Technology, Delft, The Netherlands, 2008).
3. D. Koop and C. Q. Wu, "Passive dynamic biped walking – Part I: Development and validation of an advanced model," *J. Comput. Nonlinear Dyn.* **8**(4), 041007 (2013).
4. S. Gupta and A. Kumar, "A brief review of dynamics and control of underactuated biped robots," *Adv. Robot.* **1864**(April), 1–17 (2017).
5. M. Garcia, A. Chatterjee, A. Ruina and M. Coleman, "The simplest walking model: Stability, complexity, and scaling," *J. Biomech. Eng.* **120**(2), 281–288 (1998).
6. A. L. Schwab and M. Wisse, "Basin of Attraction of the Simplest Walking Model," *Proceedings of the ASME Design Engineering Technical Conference*, Pittsburgh, Pennsylvania vol. 6 (2001) pp. 531–539.
7. M. Kwan and M. Hubbard, "Optimal foot shape for a passive dynamic biped," *J. Theor. Biol.* **248**(2), 331–339 (2007).
8. J. He and G. Ren, "On the stability of passive dynamic walker with flat foot and series ankle spring," *Adv. Mech. Eng.* **10**(3), 1–12 (2018).
9. K. E. Zelik, T.-W. P. Huang, P. G. Adamczyk and A. D. Kuo, "The role of series ankle elasticity in bipedal walking," *J. Theor. Biol.* **346**, 75–85 (2014).
10. M. Alghooneh and C. Q. Wu, "Single-support heel-off: A crucial gait event helps realizing agile and energy-efficient bipedal walking," *Robotica* **34**(6), 1335–1350 (2016).
11. Q. Wang, Y. Huang and L. Wang, "Passive dynamic walking with flat feet and ankle compliance," *Robotica* **28**(3), 413–425 (2010).
12. F. Qi, T. Wang and J. Li, "The elastic contact influences on passive walking gaits," *Robotica* **29**(5), 787–796 (2011).
13. C. Canudas de Wit, H. Olsson, K. J. Astrom and P. Lischinsky, "A new model for control of systems with friction," *IEEE Trans. Automat. Contr.* **40**(3), 419–425 (1995).
14. D. G. E. Hobbelen and M. Wisse, "A disturbance rejection measure for limit cycle walkers: The gait sensitivity norm," *IEEE T. Robot.* **23**(6), 1213–1224 (2007).
15. Y. Hürmüzlü and G. D. Moskowitz, "The role of impact in the stability of bipedal locomotion," *Dynam. Stabil. Syst.* **1**(3), 217–234 (1986).
16. A. A. Shabana, "Flexible multibody dynamics: Review of past and recent developments," *Multibody Syst. Dyn.* **1**(2), 189–222 (1997).
17. Y. Peng, Z. Zhao, M. Zhou, J. He, J. Yang and Y. Xiao, "Flexible multibody model and the dynamics of the deployment of mesh antennas," *J. Guid. Control Dyn.* **40**(6), 1499–1510 (2017).
18. O. A. Bauchau, "Flexible multibody dynamics," *Solid Mech. Appl.* **176**(4), 543–564 (2011).
19. H. Goldstein, C. Poole and J. Safko, *Classical Mechanics*, 3rd ed. (Pearson Education, Essex, England, 2011).
20. A. Shabana, *Dynamics of Multibody Systems* (Cambridge University Press, Cambridge, UK, 2005).
21. K. H. Hunt and F. R. E. Crossley, "Coefficient of restitution interpreted as damping in vibroimpact," *J Appl. Mech.* **42**(2), 440–445 (1975).
22. J. Wu, Z. Zhao and G. Ren, "Multibody analysis of the force in deploying booms," *J. Guid. Control Dyn.* **36**(6), 1881–1886 (2013).
23. E. Hairer and G. Wanner, *Solving Ordinary Differential Equations II: Stiff and Differential-algebraic Problems* (Springer, Berlin, 1996).
24. L. Ning, L. Junfeng and W. Tianshu, "The effects of parameter variation on the gaits of passive walking models: Simulations and experiments," *Robotica* **27**(4), 511–528 (2009).
25. Z. Gan, Y. Yesilevskiy, P. Zaytsev and C. D. Remy, "All common bipedal gaits emerge from a single passive model," *J R Soc Interface* **15**(146), (in press) (2018).

26. M. Kim and S. H. Collins, "Once-per-step control of ankle push-off work improves balance in a three-dimensional simulation of bipedal walking," *IEEE T. Robot.* **33**(2), 406–418 (2017).
27. D. J. J. Bregman, M. M. Van Der Krogt, V. De Groot, J. Harlaar, M. Wisse and S. H. Collins, "The effect of ankle foot orthosis stiffness on the energy cost of walking: A simulation study," *Clin. Biomech.* **26**(9), 955–961 (2011).
28. F. C. Anderson and M. G. Pandy, "A dynamic optimization solution for vertical jumping in three dimensions," *Comput. Methods Biomech. Biomed. Eng.* **2**(3), 201–231 (1999).
29. M. A. Sherman, A. Seth and S. L. Delp, "Simbody: Multibody dynamics for biomedical research," *Procedia IUTAM* **2**, 241–261 (2011).
30. D. W. Grieve, "Gait patterns and the speed of walking," *Biomed. Eng.* **3**, 119–122 (1968).
31. J. A. Nelder and R. Mead, "A simplex method for function minimization," *Comput. J.* **7**(4), 308–313 (1965).
32. M. H. Wright, *Direct Search Methods: Once Scorned, Now Respectable* (Addison-Wesley, Boston, MA, 1996) pp. 191–208.
33. S. Collins, A. Ruina, R. Tedrake and M. Wisse, "Efficient bipedal robots based on passive-dynamic walkers," *Science* **307**(5712), 1082–1085 (2005).
34. A. D. Kuo, "A simple model of bipedal walking predicts the preferred speed-step length relationship," *J. Biomech. Eng.* **123**(3), 264–269 (2001).